

# CS-AF: A Cost-sensitive Multi-classifier Active Fusion Framework for Skin Lesion Classification

Di Zhuang\*, Keyu Chen†, and J. Morris Chang‡

Department of Electrical Engineering

University of South Florida

Tampa, Florida 33620

Email: \*dizhuang@usf.edu, †keyu@usf.edu, ‡chang5@usf.edu

**Abstract**—Convolutional neural networks (CNNs) have achieved the state-of-the-art performance in skin lesion analysis. Compared with single CNN classifier, combining the results of multiple classifiers via fusion approaches shows to be more effective and robust. Since the skin lesion datasets are usually limited and statistically biased, while designing an effective fusion approach, it is important to consider not only the performance of each classifier on the training/validation dataset, but also the relative discriminative power (e.g., confidence) of each classifier regarding an individual sample in the testing phase, which calls for an active fusion approach. Furthermore, in skin lesion analysis, the data of certain classes is usually abundant making them an over-represented majority (e.g., benign lesions), while the data of some other classes is deficient, making them an underrepresented minority (e.g., cancerous lesions). It is more crucial to precisely identify the samples from an underrepresented (i.e., in terms of the amount of data) but more important (e.g., the cancerous lesions) minority class. In other words, misclassifying a more severe lesion to a benign or less severe lesion should have relative more cost (e.g., money, time and even lives). To address such challenges, we present CS-AF, a cost-sensitive multi-classifier active fusion framework for skin lesion classification. In the experimental evaluation, we prepared 60 base classifiers (of 10 CNN architectures) on the ISIC research datasets. Our experimental results show that our framework consistently outperforms the static fusion competitors.

**Index Terms**—Deep Learning, Active Fusion, Dynamic Ensemble Selection, Multi-classifier Fusion, Skin Lesion Classification.

## I. INTRODUCTION

Deep learning (DL) has achieved great success in many applications related to skin lesion analysis. For instance, Zhang et al. [1] has shown that convolutional neural networks (CNNs) have achieved the state-of-the-art performance in skin lesion classification. Also, as the development of various deep learning techniques, numerous different designs of classifiers, that might have different CNN architectures, use different sizes of the training data, use different subsets of the training data or use different feature sets, were proposed to tackle the skin lesion classification problem. For instance, as shown in the ISIC Challenges [2]–[4], several CNN architectures have been used in skin lesion analysis, including ResNet, Inception, DenseNet, PNASNet, etc.. Because of such difference (i.e., CNN architectures, subset of the training data, feature sets), those classifiers tend to have distinct performance under different conditions (e.g., different subset/classes of data). There

is no one-size-fits-all solution to design a single classifier for skin lesion classification. It is necessary to investigate multi-classifier fusion techniques to perform skin lesion classification under different conditions.

Designing an effective multi-classifier fusion approach for skin lesion classification needs to address two challenges. First, since the datasets are usually limited and statistically biased [2]–[4], while conducting multi-classifier fusion, it is necessary to consider not only the performance of each classifier on the training/validation dataset, but also the relative discriminative power (e.g., confidence) of each classifier regarding an individual sample in the testing phase. This challenge requires the researchers to design an active fusion approach, that is capable of tuning the weight assigned to each classifier dynamically and adaptively, depending on the characteristics of given samples in the testing phase. Second, since in most of the real-world skin lesion datasets [2]–[4] the data of certain classes is abundant making them an over-represented majority (e.g., benign lesions), while the data of some other classes is deficient, making them an underrepresented minority (e.g., cancerous lesions), it is more crucial to precisely identify the samples from an underrepresented (i.e., in terms of the amount of data) but more important (e.g., the cancerous lesions) minority class. For instance, a deadly cancerous lesion (e.g., a melanoma) that rarely appears during the examinations should be barely misclassified as benign or other less severe lesions (e.g., a dermatofibroma). Specifically, misclassifying a more severe lesion to a benign or less severe lesion should have relative more cost (e.g., money, time and even lives). Hence, it is also important to enable such “cost-sensitive” feature in the design of an effective multi-classifier fusion approach for skin lesion classification.

In this work, we propose CS-AF, a cost-sensitive multi-classifier active fusion framework for skin lesion classification, where we define two types of weights: the objective weights and the subjective weights. The objective weights are designed according to the classifiers’ reliability to recognize the particular skin lesions, which is determined by the prior knowledge obtained through the training phase. The subjective weights are designed according to the relative confidence of the classifiers while recognizing a specific previously “unseen” sample (i.e., individuality), which are calculated by the posterior knowledge obtained through the testing phase. While

designing the objective weights, we also utilize a customizable cost matrix to enable the “cost-sensitive” feature in our fusion framework, where given a sample, different outputs (i.e., the correct prediction or all kinds of errors) of a classifier should result in different costs. For instance, the cost of misclassifying melanoma as benign should be much higher than misclassifying benign as melanoma. In the experimental evaluation, we trained 60 classifiers as the input of our fusion framework, utilizing ten CNN architectures and three data split ratios on the ISIC research datasets for skin image analysis [2]–[4]. Our experimental results show that our CS-AF framework consistently outperforms the static fusion competitors in terms of accuracy, and always achieves lower total cost.

To summarize, our work has the following contributions:

- We present a novel and effective cost-sensitive multi-classifier active fusion framework, CS-AF. To the best of our knowledge, this is the first work to apply active fusion for skin lesion analysis.
- Our framework is the first to define the simple but effective objective/subjective weights and the customizable cost matrix, which enables the “cost-sensitive” feature for skin lesion analysis.
- A comprehensive experimental evaluation using ten popular and effective CNN architectures has been conducted on the most popular skin lesion analysis benchmark dataset, ISIC research datasets [2]–[4]. For the sake of reproducibility and convenience of future studies about fusion approaches in skin lesion analysis, we have released our prototype implementation of CS-AF, information regarding the experiment datasets and the code of our comparison experiments. \*

The rest of this paper is organized as follows: Section II presents the related literature review. Section III presents the notations of cost-sensitive active fusion, and describes our proposed framework. Section IV presents the experimental evaluation. Section V concludes.

## II. RELATED WORK

### A. Multi-classifier Fusion

Fusion approaches have been widely applied in numerous applications, such as skin lesion analysis [5], human activity recognition [6], active authentication [7], facial recognition [8]–[10], botnet detection [11]–[13] and community detection [14], [15]. According to whether the weights are dynamically/adaptively assigned to each classifier, the multi-classifier fusion approaches are divided into two categories: (i) static fusion, where the weight assigned to each participating classifier will be fixed after its initial assignment, and (ii) active fusion, where the weights are adaptively tuned depending on the characteristics of given samples in the testing phase. Many conventional approaches, such as the bagging [16], boosting [17], [18] and stacking [19], are static fusion. To date, a few methods attempting to conduct active fusion were also proposed [20]–[22]. For instance, Ren et al. [20] proposes to use the decision credibility that is evaluated by fuzzy set

theory and cloud model, to determine the real-time weight of a base classifier regarding the current sample in the testing phase. META-DES [21] defines five distinct sets of meta-features to measure the level of competence of a classifier for the classification of input samples, and proposes to train a meta-classifier to determine the rank or weight of a base classifier while facing input samples. DES-MI [22] propose an active fusion approach where the weights are determined via emphasizing more on the classifiers that are more capable of classifying examples in the region of underrepresented area among the whole sample distribution. In our work, we propose a novel active fusion approach, that leverages the “reliability” (Section III-C) and the “individuality” (Section III-D) of the base classifiers to assign the weights dynamically and adaptively.

### B. Fusion of CNNs for Skin Lesion Analysis

Convolutional neural networks (CNNs) have achieved the state-of-the-art performance [2]–[4] in skin lesion analysis since 2016 (i.e., ISIC 2016 Challenge [2]), where nearly all the teams employed CNNs in either feature extraction or classification procedure. Recently, approaches attempting to apply fusion on CNNs to tackle the skin lesion classification, are proposed [5], [23], [24]. For instance, Marchetti et al. [23] presents a fusion of CNNs framework for the classification of melanomas versus nevi or lentigines, where five fusion approaches were implemented to fuse 25 different CNN classifiers trained on the same dataset of the same problem to make a single decision. Bi et al. [24] proposes another CNNs fusion framework to tackle the classification of melanomas versus seborrheic keratosis versus nevi, where three ResNet classifiers were trained for three different classification problems via fine-tuning pretrained ImageNet CNNs: the original three-class problem and two binary classifiers (i.e., melanoma versus both other lesion classes and seborrheic carcinoma versus both other lesion classes). Perez et al. [5] conducts a comparison study between two fusion strategies for melanoma classification: selecting the classifiers at random (i.e., among 125 models over 9 CNNs architectures), and selecting the classifiers depending on their performance on a validation dataset. To summarize, most of the existing approaches use static fusion for skin lesion analysis. However, as discussed in Section I, since the skin lesion datasets are usually limited and statistically biased [2]–[4], it is necessary to enable active fusion in such problem. To the best of our knowledge, our work is the first to design and apply active fusion approach in skin lesion classification.

### C. Cost-sensitive Machine Learning

A variety of cost-sensitive machine learning approaches have been proposed to tackle the class imbalance issue in pattern classification and learning problems. Mollineda et al. [25], a comprehensive study on the class imbalance issue, divides most of the cost-sensitive machine learning approaches into two categories: the data-level and the algorithmic-level.

\*<https://tinyurl.com/tabzxec>

The data-level approaches usually manipulate the data distribution via over-sampling the samples of the minority classes or under-sampling the samples of the majority classes. For instance, SMOTE [26] is an over-sampling technique proposed to address the over-fitting problem via synthesizing more of the samples of the minority classes. Several variants of the SMOTE approach [27]–[30] are also proposed to solve this issue. The algorithmic-level approaches directly re-design the machine learning algorithms to minimize a customizable loss function, that enables the “cost-sensitive” feature, of the classifier on certain dataset (e.g., improving the sensitivity of the classifier towards minority classes). For instance, Zhang et al. [31] proposes an extreme learning machine (ELM) based evolutionary cost-sensitive classification approach, where the cost matrix would be automatically identified given a specific task (i.e., which error cost more). Iranmehr et al. [32] extends the standard loss function of support vector machine (SVM) to consider both the class imbalance (i.e., the cost) and the classification loss. Khan et al. [33] proposes a cost-sensitive deep neural network framework that could automatically learn the “cost-sensitive” feature representations for both the majority and minority classes, where during the training phase, the proposed framework would perform a joint-optimization on the class-dependent costs and the deep neural network parameters. In this work, we enable the “cost-sensitive” feature in the process of multi-classifier fusion, and employ it in the skin lesion classification problem.

### III. METHODOLOGY

#### A. Multi-classifier Fusion

In multi-classifier fusion, we define a classification space, as shown in Figure 1, where there are  $m$  classes and  $k$  classifiers. Let  $\mathcal{M} = \{M_1, M_2, \dots, M_k\}$  denote the set of base classifiers and  $\mathcal{C} = \{C_1, C_2, \dots, C_m\}$  denote the set of classes. Let  $p_{kj}^m$  denote the posterior probability of given sample  $j$  identified by classifier  $M_k$  as belonging to class  $C_m$ , where  $P_{kj} = \{p_{kj}^1, p_{kj}^2, \dots, p_{kj}^m\}$  and  $\sum_{l=1}^m p_{kj}^l = 1$ . Hence, all the posterior probabilities form a  $k \times m$  decision matrix as follows:

$$P_j = \begin{bmatrix} p_{1j}^1 & p_{1j}^2 & \cdots & p_{1j}^m \\ p_{2j}^1 & p_{2j}^2 & \cdots & p_{2j}^m \\ \vdots & \vdots & \ddots & \vdots \\ p_{kj}^1 & p_{kj}^2 & \cdots & p_{kj}^m \end{bmatrix} \quad (1)$$

Since the importance of different classifiers might be different, we assign a weight  $w_i$  to the decision vector (i.e., posterior probabilities vector) of each classifier  $C_i$ , where  $i \in \{1, 2, \dots, k\}$ . Let  $P_m(j)$  denote the sum of the posterior probabilities, that sample  $j$  belonging to class  $m$ , of all the classifiers. Then, we have

$$P_m(j) = \sum_{i=1}^k w_i \cdot p_{ij}^m \quad (2)$$

The final decision (i.e., class)  $D(j)$  of sample  $j$  is determined by the maximum posterior probabilities sum:

$$D(j) = \max_i P_i(j), \quad i \in \{1, 2, \dots, m\} \quad (3)$$

Conventional multi-classifier fusion approaches either use the same weight for all the classifiers (i.e., average fusion) or use static weights that will not be changed after its initial assignment during the training phase. As illustrated in Figure 1, our weights (i.e.,  $w_k = \alpha \cdot O_k + (1 - \alpha) \cdot S_k$ ) contains two components: (i) the objective weight  $O_k$  that is static and determined by the prior knowledge obtained through the training phase (Section III-C), and (ii) the subjective weight  $S_k$  that is dynamic and calculated by the posterior knowledge obtained through the testing phase (Section III-D). We use a predefined hyper-parameter  $\alpha$  to tune the emphasis on either  $O_k$  or  $S_k$ , while combining them together.

#### B. Cost-sensitive Problem Formulation

As discussed in Section I, given a sample, different outputs (i.e., the correct prediction or all kinds of errors) of a classifier should result in different costs. For instance, misclassifying a more severe lesion to a benign or less severe lesion should have relative higher cost. Let  $c_{pq}$  denote the cost of classifying an instance belonging to class  $p$  into class  $q$ . Then, we obtain a cost matrix as follows:

$$CM = \begin{bmatrix} c_{11} & c_{12} & \cdots & c_{1m} \\ c_{21} & c_{22} & \cdots & c_{2m} \\ \vdots & \vdots & \ddots & \vdots \\ c_{m1} & c_{m2} & \cdots & c_{mm} \end{bmatrix} \quad (4)$$

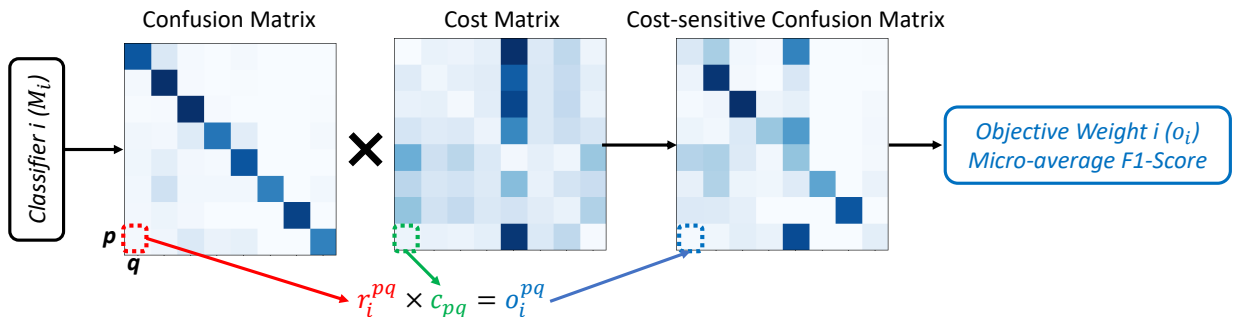
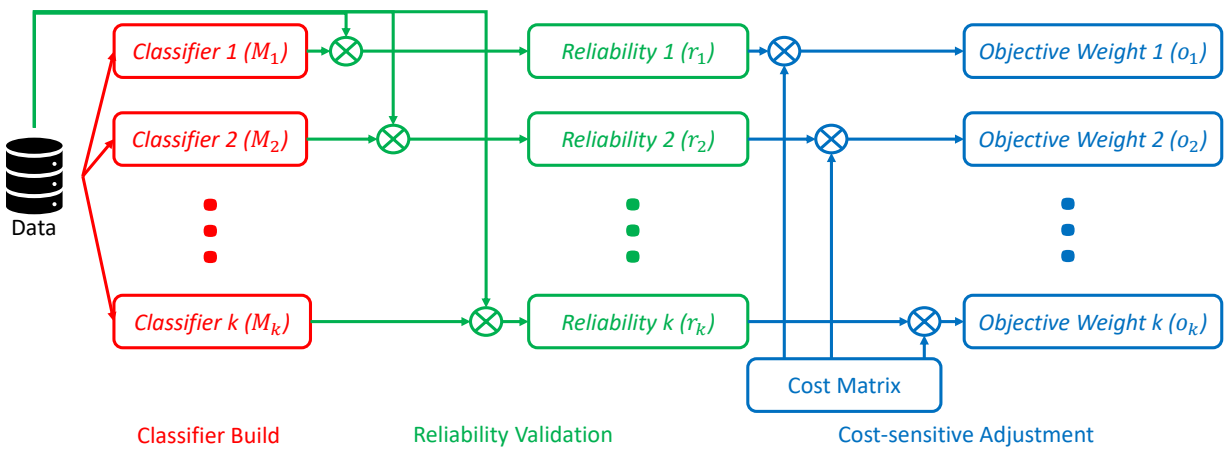
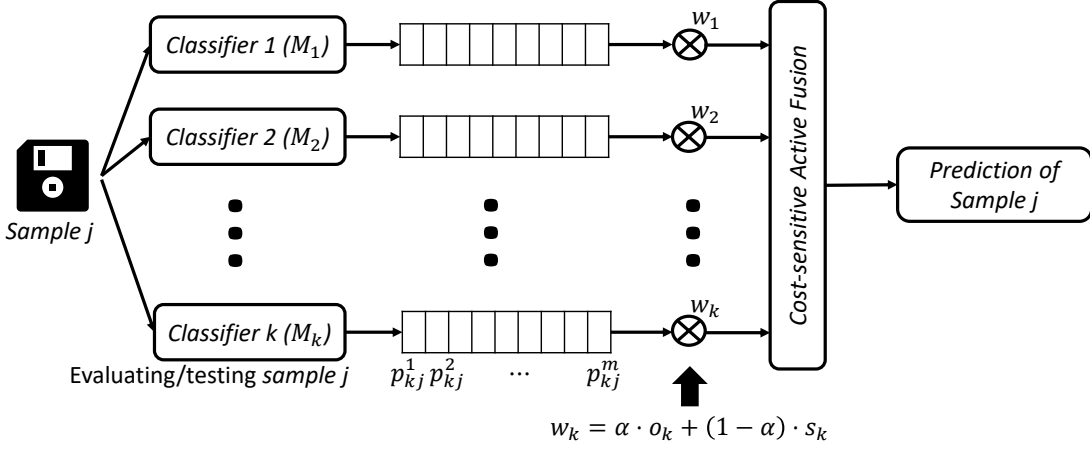
Let  $W = \{w_1, w_2, \dots, w_k\}$  be a fusion weight vector, and  $\mathcal{W}$  be the fusion weight vector space, where  $W \in \mathcal{W}$ . The goal of cost-sensitive multi-classifier fusion is to find the  $W^* \in \mathcal{W}$ , that can minimize the average cost of the fusion approach’s outcomes over all the testing samples. In Section IV-C, we provide certain principles to design a good cost matrix, and provided one based on our literature references and those principles.

#### C. Computing the Objective Weights

The objective weights are designed according to the classifiers reliability to recognize the particular skin lesions, which is determined by the prior knowledge obtained through the training phase. In the training phase, we separate all the labelled data into two parts: training data and validation data. As shown in Figure 2, computing the objective weights in our framework contains three steps:

- Classifier build. We prepare a set of base classifiers, where all the classifiers might have different CNN architectures, use different size of the training data, or use different subset of the training data. In this step, we trained 60 base classifiers, more details are introduced in Section IV-B.

- Reliability validation. Let  $r_i$  denote the reliability of a base classifier  $M_i$ , that is designed to describe the average recognition performance of the classifier on the validation data.



Higher accuracy and less error on the validation data usually means higher reliability. Hence, we use the confusion matrix result of each base classifier on the same validation dataset as its reliability, where a confusion matrix [34] is a table that is often used to describe the performance of a classifier on a set of validation data for which the true values are known. It allows easy identification of confusion between classes, e.g., one class is commonly mislabeled as the other. Many performance measures could be computed from the confusion

matrix (e.g., F-scores). As such, we use  $r_i^{pq}$  to denote the probability of a base classifier  $M_i$  classifying an instance belonging to class p into class q.

- Cost-sensitive adjustment. As described in Section III-B, we would like to enable the “cost-sensitive” feature in the design of our objective weights. As shown in Figure 4, for each classifier  $M_i$ , we use an element-wise multiplication between its reliability  $r_i$  (confusion matrix) and the customized cost matrix (Section III-B) to formulate a cost-sensitive confusion

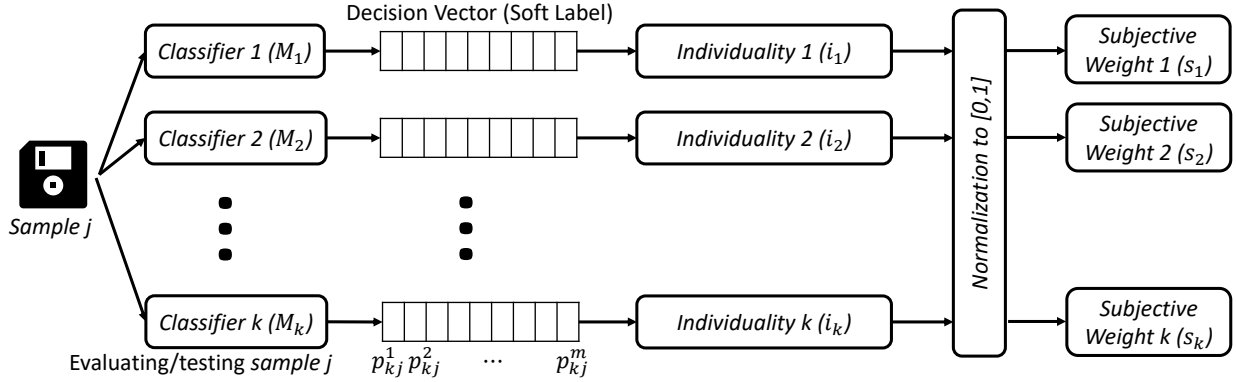


Fig. 4: The calculation of subjective weights.

matrix, where all the results/errors in the confusion matrix have been adjusted based on the cost matrix. Then, we use the micro-average F1-score [35] of the cost-sensitive confusion matrix to define the objective weight of each base classifier, and all the object weights are automatically normalized to  $(0, 1]$ .

#### D. Computing the Subjective Weights

The subjective weights are designed according to the relative confidence of the classifiers while recognizing a specific previously unseen image (i.e., individuality), which are calculated by the posterior knowledge obtained through the testing phase. As shown in Figure 4, computing the subjective weights in our framework contains three steps:

- Sample evaluating/testing. Each sample is evaluated/tested through all the classifiers to obtain the corresponding decision vectors (i.e., the soft labels).

- Individuality calculation. We consider the individuality of a classifier as its relative class discriminative power regarding a given individual sample. A classifier can easily identify the class of a given sample in the testing phase, if its posterior probabilities of the corresponding decision vector is highly concentrated in one class, and the misclassification rate would also be low. On the contrary, if the distribution of the posterior probabilities is close to uniform, the classifier shows its difficulty in discriminating the class of the given sample. Also, different classifiers would present different distribution of the posterior probabilities in the decision vectors while testing the same sample. Hence, we define the individuality  $i_k^*$  of a classifier  $M_k$  using the posterior probabilities distribution as follows:

$$i_k^* = \frac{1}{m-1} \sum_{l=1}^m (p_{kj}^* - p_{kj}^l) \quad (5)$$

where  $p_{kj}^*$  is the largest posterior probability value in  $P_{kj}$ .

- Normalization. Since the individualities are relative values among all the base classifiers, we normalize each individuality  $i_k^*$  to  $i_k \in [0, 1]$  as follows:

$$i_k = \frac{i_k^* - i_{min}}{i_{max} - i_{min}} \quad (6)$$

where  $i^{min} = \min_{j \in 1, 2, \dots, k} i_j^*$  and  $i^{max} = \max_{j \in 1, 2, \dots, k} i_j^*$ .

## IV. EXPERIMENTAL EVALUATION

We conducted our experiments on the ISIC Challenge 2019 dataset [3], [36], [37] and 10 CNN architectures to evaluate the performance of our proposed CS-AF framework. Comparisons have been made among Max-Voting Fusion (static), Average Fusion (static), AF (i.e., active fusion that does not have the “cost-sensitive” feature) and our CS-AF framework. The presented results show that our approach consistently better than base static fusion approaches (i.e., Max-Voting and Average Fusion) in terms of the accuracy and provide lower cost.

### A. Experiment Dataset

In our experiments, we utilized the well known skin image dataset: ISIC Challenge 2019 [3], [36], [37]. Since the ground truth of the test data was not available, we only employed the training data in our evaluation and without meta-data. This dataset contains 25,331 images, taken from 3 source datasets: BCN\_20000 [36], HAM10000 [37] and MSK [3]. It depicts 8 skin lesion diseases (i.e., 8 classes): melanoma (4,522), melanocytic nevus (12,875), basal cell carcinoma (3,323), actinic keratosis (867), benign keratosis (2624), dermatofibroma (239), vascular lesion (253) and squamous cell carcinoma (628).

We randomly select 5% and 15% from the entire datasets as the validation and testing dataset, respectively. For the rest 80% dataset, we produced 6 training datasets: (i) one full training set that contains the entire 80% dataset (25,331), (ii) two sub-70 training sets that each contains 70% (i.e., randomly selected) of the full training set, and (iii) three sub-60 training sets that each contains 60% (i.e., randomly selected) of the full training set. Since the numbers of samples of different classes are extremely unbalanced, in order to keep most of the information of each disease, we retained all images of the classes that each has less than 1,000 images while creating the sub-70 and sub-60 datasets.

### B. Base Classifiers Preparation

We evaluated 10 different CNN architectures (Table I) with parameters pre-trained on ImageNet [46]. All the networks

TABLE I: The performance (accuracy in %) of the base classifiers of ten CNN architectures. (Full indicates the performance on full training set. Sub-70 and Sub-60 indicate the performance on 70% and 60% of the full training set.)

CNN Architectures	Full	Sub-70	Sub-60
PNASNet-5-Large [38]	87.87	$86.60 \pm 0.14$	$84.88 \pm 0.13$
NASNet-A-Large [39]	87.79	$85.91 \pm 0.01$	$84.34 \pm 0.09$
ResNeXt101-32 $\times$ 16d [40]	87.76	$85.37 \pm 0.05$	$84.12 \pm 0.08$
SENet154 [41]	88.00	$85.26 \pm 0.01$	$84.38 \pm 0.08$
Dual Path Net-107 [42]	86.23	$82.32 \pm 0.08$	$82.23 \pm 0.03$
Xception [43]	87.18	$83.93 \pm 0.02$	$83.40 \pm 0.06$
Inception-V4 [44]	85.99	$83.44 \pm 0.13$	$82.05 \pm 0.07$
InceptionResNet-V2 [44]	87.53	$84.18 \pm 0.01$	$82.39 \pm 0.10$
SE-ResNeXt101-32 $\times$ 4d [41]	87.55	$84.78 \pm 0.01$	$83.67 \pm 0.08$
ResNet152 [45]	84.00	$82.59 \pm 0.03$	$81.76 \pm 0.14$

expected input images to be:  $331 \times 331$  for PNASNet-5-Large and NASNet-A-Large;  $320 \times 320$  for ResNeXt101-32 $\times$ 16d;  $299 \times 299$  for Xception, Inception-V4 and InceptionResNet-V2;  $224 \times 224$  for SENet154, Dual Path Net-107, SE-ResNeXt101-32 $\times$ 4d and ResNet152. The networks were finetuned by stochastic gradient decent (SGD) with learning rate  $10^{-3}$  and momentum 0.9. The learning rate degraded in 20 epochs by 0.1. We stopped the training process either after 40 epochs or the validation accuracy failed to improve for 7 consecutive epochs. Data augmentation was also adopted in our experiment, by random horizontal flipping with probability 0.5 and random rotation up to 90 degrees. Our experiments were implemented using Pytorch, running on a server with 4 GTX 1080Ti 11 GB GPUs. To keep the same batch size 32 in each evaluation, and due to the memory constraint of single GPU, certain networks were trained with several GPUs: PNASNet (4), NASNet (4), ResNext (4), Dual Path Net (2) and SENet (2). Table I shows the performance of the base classifiers on the testing dataset, while trained on the full, sub-70 and sub-60, respectively.

### C. Design of the Cost Matrix

As discussed in Section III-B, it is necessary to have a good cost matrix to enable our “cost-sensitive” feature in our active fusion framework. As such, we create several principles to design an adequate cost matrix: (i) All the costs should be positive, since it will be item-wise multiplied with the confusion matrix, and we don’t want to get non-positive values in our cost-sensitive confusion matrix. (ii) The cost of the correct predictions should depend on the severeness of the corresponding disease. For instance, it should be more valuable (i.e., less cost) to classify a more severe disease (i.e., melanoma) correctly. (iii) The cost of correct predictions should be no more than the cost of incorrect predictions. (iv) The relative costs of different incorrect predictions should be based on their relative severeness. For instance, misclassifying melanoma (i.e., a deadly cancerous lesion) as benign keratosis should result in much more cost than the opposite scenario.

	1	14	12	18	192	27	53	10
Mel	12	4	9	11	79	14	24	10
Mel-Nv	10	11	3	13	111	18	32	9
BCC	14	10	11	5	53	12	18	13
AK	136	57	79	39	8	25	14	106
BK	21	12	14	10	32	6	13	17
Der	39	19	25	14	18	11	7	31
VL	9	12	10	15	148	22	42	2
SCC	Mel	Mel-Nv	BCC	AK	BK	Der	VL	SCC

Fig. 5: Cost Matrix for Skin Lesion Classification

To figure out the relative severeness relationships among all eight skin lesion classes and better design our cost matrix, we also refer to some literature regarding to the severeness of those diseases [47]–[55]. As such, we design our example cost matrix to demo our work, as illustrated in Figure 5. The other researchers could also create the cost matrix with their own demands or based on their own best domain expert knowledge.

### D. Effectiveness Analysis

In this section, we conducted a comparison between CS-AF and three other fusion methods. **Max-Voting Fusion** is a static approach, where it combines predictions from base classifiers and only the sample class with the highest votes will be included in the final prediction. **Average Fusion** is another static approach, where it averages decision vectors of base classifiers and uses the averaged decision vector to make the final prediction. **AF** is a baseline active fusion approach by removing the cost-sensitive adjustment step from CS-AF while calculating the objective weights.

To evaluate the effectiveness and consistency of CS-AF. We randomly picked certain number of classifiers among our 60 base classifiers, and compute the fusion accuracy and the total cost, where the total cost was calculated by the item-wise product between the testing confusion matrix and our cost matrix. The results (shown in Figure 6) were averaged over 100 repetitions along with the variance, and with two different  $\alpha$  values 0.3 and 0.7, as introduced in Section III-A. From the results, we observe that: (i) For all fusion methods, with more base classifiers involved, the accuracy tends to increase and the total cost tends to decrease. (ii) The total cost variance of CS-AF and AF were less when  $\alpha = 0.7$  (compared with when  $\alpha = 0.3$ ), since higher  $\alpha$  weights more on the objective weights that include the “cost-sensitive” feature. (iii) While using different  $\alpha$  values, our methods consistently got higher accuracy and lower total cost than the static fusion competitors. The difference was slightly larger when  $\alpha = 0.7$ . (iv) The accuracy ( $\alpha = 0.7$ ) of CS-AF is consistently 0.5%

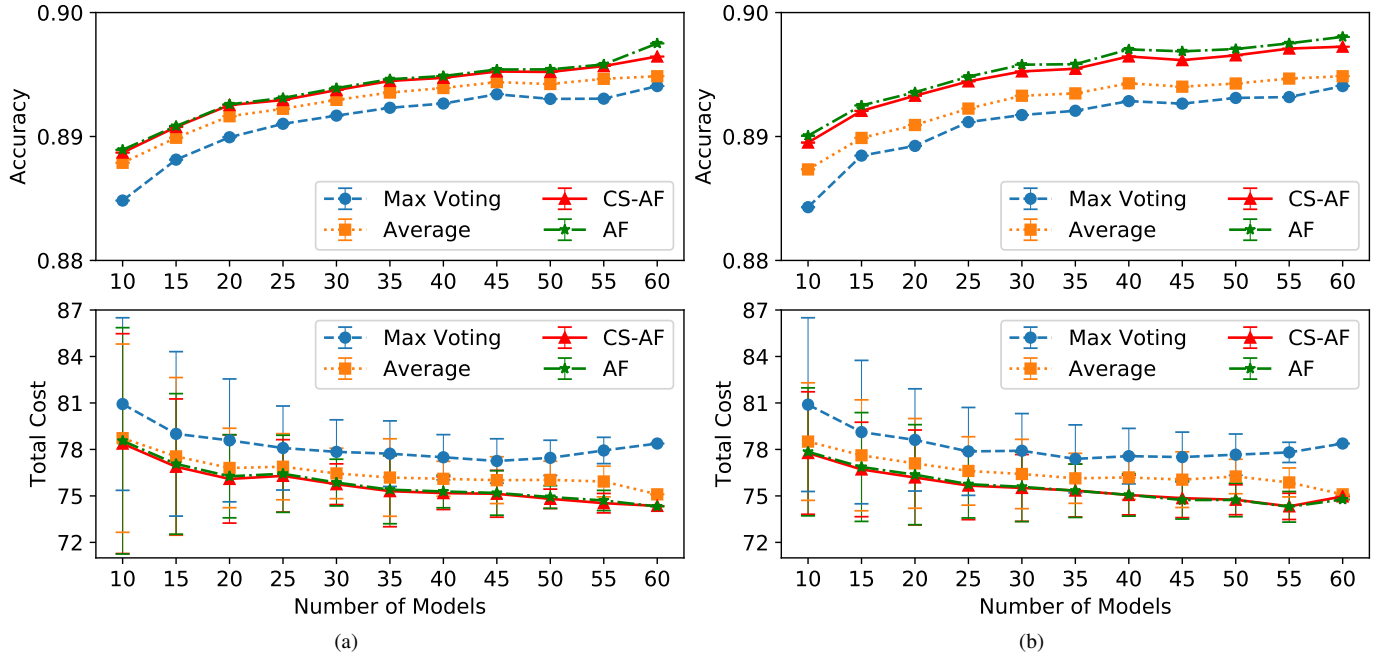


Fig. 6: Comparison experiments with fusion of classifiers. (a)  $\alpha = 0.3$ . (b)  $\alpha = 0.7$ .

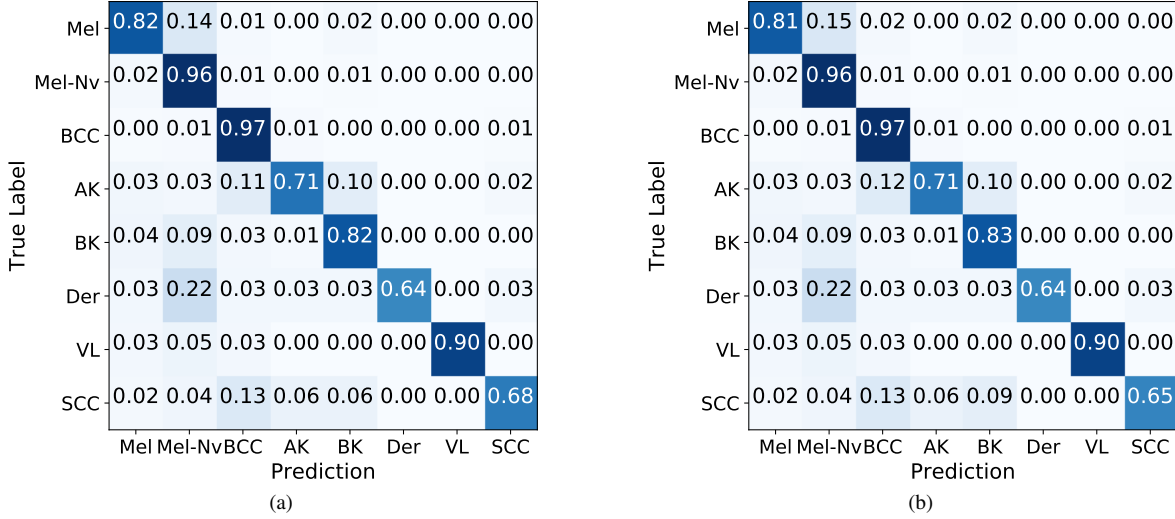


Fig. 7: The confusion matrices on the testing dataset when  $\alpha = 0.7$ . (a) CS-AF with accuracy 90.57% and total cost 77.74. (b) Average Fusion with accuracy 90.47% and total cost 82.10.

and 0.2% higher than Max-Voting and Average Fusion, while the cost is consistently 2.6 and 1 lower than the results of those two methods, respectively. (v) CS-AF has slightly lower overall accuracy than AF got, while also achieves slightly lower cost.

We also compared the confusion matrices of CS-AF ( $\alpha = 0.7$ ) and Average Fusion. Both of them were implemented on the 10 best models of different CNN architectures (second column of Table I). As shown in Figure 7, although the confusion matrices were very close, if we combine them with

the cost matrix (Figure 5), we can find that the difference of the total costs was mainly caused by the misclassifying of SCC (squamous cell carcinoma) to AK (actinic keratosis). The 3% less incorrect prediction of CS-AF leads to its 4.4 less total cost compared with the Average Fusion.

## V. CONCLUSION

In this paper, we propose CS-AF, a cost-sensitive multi-classifier active fusion framework for skin lesion classification, where we define two types of weights: the objective weights

that are designed according to the classifiers reliability to recognize the particular skin lesions, and the subjective weights that are designed according to the relative confidence of the classifiers while recognizing a specific previously unseen image (i.e., individuality). We also enable the “cost-sensitive” feature in our framework, via incorporating a customizable cost matrix in the design of the objective weights. In the experimental evaluation, we trained 60 classifiers of ten CNN architectures as the base classifiers, and compared our CS-AF framework with two static fusion approaches (i.e., Max-Voting Fusion and Average Fusion), and a baseline active fusion approach, AF. Our experimental results show that our CS-AF framework consistently outperforms the static fusion competitors in terms of accuracy, and always achieves lower total cost. In our future work, we plan to (i) investigate and incorporate other metrics (i.e., other than F1-score) in the design of the objective weights; (ii) design learning-based approach to determine the subjective weights; and (iii) employ and evaluate our CS-AF framework in other medicine-related applications.

#### ACKNOWLEDGMENTS

Effort sponsored in whole or in part by United States Special Operations Command (USSOCOM), under Partnership Intermediary Agreement No. H92222-15-3-0001-01. The U.S. Government is authorized to reproduce and distribute reprints for Government purposes notwithstanding any copyright notation thereon. \*

#### REFERENCES

- [1] J. Zhang, Y. Xie, Y. Xia, and C. Shen, “Attention residual learning for skin lesion classification,” *IEEE transactions on medical imaging*, vol. 38, no. 9, pp. 2092–2103, 2019.
- [2] D. Gutman, N. C. Codella, E. Celebi, B. Helba, M. Marchetti, N. Mishra, and A. Halpern, “Skin lesion analysis toward melanoma detection: A challenge at the international symposium on biomedical imaging (isbi) 2016, hosted by the international skin imaging collaboration (isic),” *arXiv preprint arXiv:1605.01397*, 2016.
- [3] N. C. Codella, D. Gutman, M. E. Celebi, B. Helba, M. A. Marchetti, S. W. Dusza, A. Kalloo, K. Liopyris, N. Mishra, H. Kittler *et al.*, “Skin lesion analysis toward melanoma detection: A challenge at the 2017 international symposium on biomedical imaging (isbi), hosted by the international skin imaging collaboration (isic),” in *2018 IEEE 15th International Symposium on Biomedical Imaging (ISBI 2018)*. IEEE, 2018, pp. 168–172.
- [4] N. Codella, V. Rotemberg, P. Tschandl, M. E. Celebi, S. Dusza, D. Gutman, B. Helba, A. Kalloo, K. Liopyris, M. Marchetti *et al.*, “Skin lesion analysis toward melanoma detection 2018: A challenge hosted by the international skin imaging collaboration (isic),” *arXiv preprint arXiv:1902.03368*, 2019.
- [5] F. Perez, S. Avila, and E. Valle, “Solo or ensemble? choosing a cnn architecture for melanoma classification,” in *Proceedings of the IEEE Conference on Computer Vision and Pattern Recognition Workshops*, 2019, pp. 0–0.
- [6] D. Tao, L. Jin, Y. Yuan, and Y. Xue, “Ensemble manifold rank preserving for acceleration-based human activity recognition,” *IEEE transactions on neural networks and learning systems*, vol. 27, no. 6, pp. 1392–1404, 2014.
- [7] P.-Y. Wu, C.-C. Fang, J. M. Chang, and S.-Y. Kung, “Cost-effective kernel ridge regression implementation for keystroke-based active authentication system,” *IEEE transactions on cybernetics*, vol. 47, no. 11, pp. 3916–3927, 2016.
- [8] C. Ding and D. Tao, “Trunk-branch ensemble convolutional neural networks for video-based face recognition,” *IEEE transactions on pattern analysis and machine intelligence*, vol. 40, no. 4, pp. 1002–1014, 2017.
- [9] H. Nguyen, D. Zhuang, P.-Y. Wu, and M. Chang, “Autogan-based dimension reduction for privacy preservation,” *Neurocomputing*, 2019.
- [10] D. Zhuang, S. Wang, and J. M. Chang, “Fripal: Face recognition in privacy abstraction layer,” in *2017 IEEE Conference on Dependable and Secure Computing*. IEEE, 2017, pp. 441–448.
- [11] L. Mai and D. K. Noh, “Cluster ensemble with link-based approach for botnet detection,” *Journal of Network and Systems Management*, vol. 26, no. 3, pp. 616–639, 2018.
- [12] D. Zhuang and J. M. Chang, “Peerhunter: Detecting peer-to-peer botnets through community behavior analysis,” in *2017 IEEE Conference on Dependable and Secure Computing*. IEEE, 2017, pp. 493–500.
- [13] —, “Enhanced peerhunter: Detecting peer-to-peer botnets through network-flow level community behavior analysis,” *IEEE Transactions on Information Forensics and Security*, vol. 14, no. 6, pp. 1485–1500, 2018.
- [14] A. Tagarelli, A. Amelio, and F. Gullo, “Ensemble-based community detection in multilayer networks,” *Data Mining and Knowledge Discovery*, vol. 31, no. 5, pp. 1506–1543, 2017.
- [15] D. Zhuang, M. J. Chang, and M. Li, “Dynamo: Dynamic community detection by incrementally maximizing modularity,” *IEEE Transactions on Knowledge and Data Engineering*, 2019.
- [16] L. Breiman, “Bagging predictors,” *Machine learning*, vol. 24, no. 2, pp. 123–140, 1996.
- [17] R. E. Schapire, “The strength of weak learnability,” *Machine learning*, vol. 5, no. 2, pp. 197–227, 1990.
- [18] Y. Freund and R. E. Schapire, “A desicion-theoretic generalization of on-line learning and an application to boosting,” in *European conference on computational learning theory*. Springer, 1995, pp. 23–37.
- [19] D. H. Wolpert, “Stacked generalization,” *Neural networks*, vol. 5, no. 2, pp. 241–259, 1992.
- [20] F. Ren, Y. Li, and M. Hu, “Multi-classifier ensemble based on dynamic weights,” *Multimedia Tools and Applications*, vol. 77, no. 16, pp. 21 083–21 107, 2018.
- [21] R. M. Cruz, R. Sabourin, G. D. Cavalcanti, and T. I. Ren, “Meta-des: A dynamic ensemble selection framework using meta-learning,” *Pattern recognition*, vol. 48, no. 5, pp. 1925–1935, 2015.
- [22] S. García, Z.-L. Zhang, A. Albalhi, S. Alshomrani, and F. Herrera, “Dynamic ensemble selection for multi-class imbalanced datasets,” *Information Sciences*, vol. 445, pp. 22–37, 2018.
- [23] M. A. Marchetti, N. C. Codella, S. W. Dusza, D. A. Gutman, B. Helba, A. Kalloo, N. Mishra, C. Carrera, M. E. Celebi, J. L. DeFazio *et al.*, “Results of the 2016 international skin imaging collaboration international symposium on biomedical imaging challenge: Comparison of the accuracy of computer algorithms to dermatologists for the diagnosis of melanoma from dermoscopic images,” *Journal of the American Academy of Dermatology*, vol. 78, no. 2, pp. 270–277, 2018.
- [24] L. Bi, J. Kim, E. Ahn, and D. Feng, “Automatic skin lesion analysis using large-scale dermoscopy images and deep residual networks,” *arXiv preprint arXiv:1703.04197*, 2017.
- [25] R. Mollineda, R. Alejo, and J. Sotoca, “The class imbalance problem in pattern classification and learning,” in *II Congreso Espanol de Informática (CEDI 2007)*. ISBN, 2007, pp. 978–84.
- [26] N. V. Chawla, K. W. Bowyer, L. O. Hall, and W. P. Kegelmeyer, “Smote: synthetic minority over-sampling technique,” *Journal of artificial intelligence research*, vol. 16, pp. 321–357, 2002.
- [27] K.-J. Wang, B. Makond, K.-H. Chen, and K.-M. Wang, “A hybrid classifier combining smote with pso to estimate 5-year survivability of breast cancer patients,” *Applied Soft Computing*, vol. 20, pp. 15–24, 2014.
- [28] H. Han, W.-Y. Wang, and B.-H. Mao, “Borderline-smote: a new oversampling method in imbalanced data sets learning,” in *International conference on intelligent computing*. Springer, 2005, pp. 878–887.
- [29] C. Bunkhumpornpat, K. Sinapiromsaran, and C. Lursinsap, “Safe-level-smote: Safe-level-synthetic minority over-sampling technique for handling the class imbalanced problem,” in *Pacific-Asia conference on knowledge discovery and data mining*. Springer, 2009, pp. 475–482.

\*The views and conclusions contained herein are those of the authors and should not be interpreted as necessarily representing the official policies or endorsements, either expressed or implied, of the United States Special Operations Command.

[30] T. Maciejewski and J. Stefanowski, "Local neighbourhood extension of smote for mining imbalanced data," in *2011 IEEE Symposium on Computational Intelligence and Data Mining (CIDM)*. IEEE, 2011, pp. 104–111.

[31] L. Zhang and D. Zhang, "Evolutionary cost-sensitive extreme learning machine," *IEEE transactions on neural networks and learning systems*, vol. 28, no. 12, pp. 3045–3060, 2016.

[32] A. Iranmehr, H. Masnadi-Shirazi, and N. Vasconcelos, "Cost-sensitive support vector machines," *Neurocomputing*, vol. 343, pp. 50–64, 2019.

[33] S. H. Khan, M. Hayat, M. Bennamoun, F. A. Sohel, and R. Togneri, "Cost-sensitive learning of deep feature representations from imbalanced data," *IEEE transactions on neural networks and learning systems*, vol. 29, no. 8, pp. 3573–3587, 2017.

[34] S. Visa, B. Ramsay, A. L. Ralescu, and E. Van Der Knaap, "Confusion matrix-based feature selection," *MAICS*, vol. 710, pp. 120–127, 2011.

[35] V. Van Asch, "Macro-and micro-averaged evaluation measures [[basic draft]]," *Belgium: CLIPS*, vol. 49, 2013.

[36] M. Combalia, N. C. Codella, V. Rotemberg, B. Helba, V. Vilaplana, O. Reiter, A. C. Halpern, S. Puig, and J. Malvehy, "Bcn20000: Dermoscopic lesions in the wild," *arXiv preprint arXiv:1908.02288*, 2019.

[37] P. Tschandl, C. Rosendahl, and H. Kittler, "The ham10000 dataset, a large collection of multi-source dermatoscopic images of common pigmented skin lesions," *Scientific data*, vol. 5, p. 180161, 2018.

[38] C. Liu, B. Zoph, M. Neumann, J. Shlens, W. Hua, L.-J. Li, L. Fei-Fei, A. Yuille, J. Huang, and K. Murphy, "Progressive neural architecture search," in *Proceedings of the European Conference on Computer Vision (ECCV)*, 2018, pp. 19–34.

[39] B. Zoph and Q. V. Le, "Neural architecture search with reinforcement learning," *arXiv preprint arXiv:1611.01578*, 2016.

[40] S. Xie, R. Girshick, P. Dollár, Z. Tu, and K. He, "Aggregated residual transformations for deep neural networks," in *Proceedings of the IEEE conference on computer vision and pattern recognition*, 2017, pp. 1492–1500.

[41] J. Hu, L. Shen, and G. Sun, "Squeeze-and-excitation networks," in *Proceedings of the IEEE conference on computer vision and pattern recognition*, 2018, pp. 7132–7141.

[42] Y. Chen, J. Li, H. Xiao, X. Jin, S. Yan, and J. Feng, "Dual path networks," in *Advances in neural information processing systems*, 2017, pp. 4467–4475.

[43] F. Chollet, "Xception: Deep learning with depthwise separable convolutions," in *Proceedings of the IEEE conference on computer vision and pattern recognition*, 2017, pp. 1251–1258.

[44] C. Szegedy, S. Ioffe, V. Vanhoucke, and A. A. Alemi, "Inception-v4, inception-resnet and the impact of residual connections on learning," in *Thirty-first AAAI conference on artificial intelligence*, 2017.

[45] K. He, X. Zhang, S. Ren, and J. Sun, "Deep residual learning for image recognition," in *Proceedings of the IEEE conference on computer vision and pattern recognition*, 2016, pp. 770–778.

[46] J. Deng, W. Dong, R. Socher, L.-J. Li, K. Li, and L. Fei-Fei, "ImageNet: A Large-Scale Hierarchical Image Database," in *CVPR09*, 2009.

[47] "Whats the difference between melanoma and skin cancer?" 2020. [Online]. Available: <https://blog.dana-farber.org/insight/2019/12/difference-between-melanoma-and-skin-cancer/>

[48] "What are the prognosis and survival rates for melanoma by stage?" 2020. [Online]. Available: <https://www.healthline.com/health/melanoma-prognosis-and-survival-rates>

[49] "Mole," 2020. [Online]. Available: <https://dermnetnz.org/topics/mole/>

[50] "Skin cancer," 2020. [Online]. Available: <https://www.webmd.com/melanoma-skin-cancer/skin-cancer#1-1>

[51] "Understanding actinic keratosis – the basics," 2020. [Online]. Available: <https://www.webmd.com/skin-problems-and-treatments/understanding-actinic-keratosis-basics>

[52] "Seborrheic keratosis," 2020. [Online]. Available: <https://www.mayoclinic.org/diseases-conditions/seborrheic-keratosis/symptoms-causes/syc-20353878>

[53] "Surgery for vascular malformations in the torso & limbs," 2020. [Online]. Available: <https://nyulangone.org/conditions/vascular-malformations-in-the-torso-limbs-in-adults/treatments/surgery-for-vascular-malformations-in-the-torso-limbs>

[54] "Types of vascular malformations in the torso & limbs," 2020. [Online]. Available: <https://nyulangone.org/conditions/vascular-malformations-in-the-torso-limbs-in-adults/types>

[55] "Basal cell carcinoma and squamous cell carcinoma," 2020. [Online]. Available: <http://www.ucsfhealth.org/conditions/basal-cell-and-squamous-cell-carcinoma>